DECISION–FEEDBACK DIFFERENTIAL DEMODULATION OF BIT–INTERLEAVED CODED MDPSK FOR FLAT RAYLEIGH FADING CHANNELS

Lutz H.-J. Lampe and Robert Schober

Laboratorium für Nachrichtentechnik, Universität Erlangen–Nürnberg
Cauerstraße 7, D–91058 Erlangen, Germany
e-mail: {*LLampe,schober*}*@LNT.de*, WWW: *http://www.LNT.de/LNT2*

***Abstract* — A novel simple receiver structure for M-ary differential phase–shift keying (MDPSK) transmission over flat Rayleigh fading channels without channel state information is proposed. We apply convolutional codes for error correction and bit–interleaving as appropriate means to combat the effects of fading. In the decoding the hard decisions of the Viterbi algorithm are fed back to enable a more reliable estimation of the current channel state. A theoretical analysis of the associated cutoff rate for error–free feedback shows remarkable gains in power efficiency compared to conventional differential demodulation, while the computational complexity of the decoding remains low. The results from information theory are in good agreement with the obtained simulation results. The proposed scheme works remarkably well for target bit error rates which are usually of interest.**

1. Introduction

Digital receivers performing noncoherent detection are very attractive because of their robustness against ambiguities and impairment of the phase of the received signal. In particular, reliable estimation of the carrier phase and, in the case of transmission over fading channels, the current channel state is often not practicable. However, usually the underlying channel can be assumed to be slowly time–variant or even time–invariant over at least two consecutive symbols. The resulting dependences among the received symbols should be utilized in the receiver processing in order to improve performance.
Consequently, in state–of–the–art noncoherent receivers the decision variables are based on several received symbols within an observation interval of $N \geq 2$ symbols. In this way, for the additive white Gaussian noise (AWGN) channel with constant (unknown) phase it has been shown that the performance of coherent transmission is approached if N is chosen sufficiently large N , cf. e.g. [1, 2, 3]. However, the larger N is chosen the more complex the receiver becomes.
If differential encoding or some other modulation code, cf. e.g. [4, 5], succeeds the channel encoder to avoid the problem of phase ambiguity, iterative decoding schemes regarding the modulation as inner component code of a serially concatenated code have been proposed in e.g. [4, 6, 7, 8, 9]. Soft decisions of the outer (error correcting code) decoder are fed back to the inner decoder to improve the delivered decision values. Here, computational complexity increases exponentially with N and linearly with the number of iterations.
In this paper, we propose a novel noncoherent receiver with a very low computational complexity for M–ary differential phase–shift keying (MDPSK) transmission with convolutional codes for error correction coding over flat Rayleigh fading channels. In particular, we apply an iterative decoding procedure, where the *hard* decisions of the Viterbi algorithm are fed back in order to enable demodulation based on an extended observation interval N. This decision–feedback differential demodulation (DF–DM) approach can be regarded as analogous to decision–feedback differential detection (DF–DD) for uncoded transmission, e.g. [10, 11]. Although the incorporation of hard decisions in the iterative decoding procedure is clearly suboptimum, performance gains of several dBs compared to conventional differential demodulation are achieved, while receiver complexity increases only moderately and is almost independent of N.
In order to mitigate the effects of fading, we apply bit–wise interleaving. This bit–interleaved coded modulation (BICM) has been proved to be very effective for the flat Rayleigh fading channel [12, 13]. Noteworthy, non–iterative reduced complexity decoding schemes, which have been proposed in [14, 15], do not allow the inclusion of interleaving.
It should be mentioned that an iterative decoding technique with hard decision–feedback has also been proposed in [16]. There, regarding the mapping as a modulation code enables an improvement of the performance of BICM with iterative coherent demodulation.

2. System Model

The block diagram of the discrete–time system model in the equivalent low–pass domain is depicted in Figure 1. The convolutional encoder output symbols $c[i]$ ($i \in \mathbb{Z}$: bit discrete–time index) are bit–wise interleaved, and $\ell \triangleq \log_2(M)$ interleaved coded bits are mapped ($\mathcal{M}(\cdot)$) to M–ary PSK data–carrying symbols $a[k]$ ($k \in \mathbb{Z}$: symbol discrete–time index). In order to enable noncoherent demodulation, $a[k]$ is differentially encoded, i.e., $x[k] = a[k] \cdot x[k-1]$.
We assume sufficiently slow fading, i.e., the channel does not change significantly during one symbol interval, and transmitter and receiver filters with square–root Nyquist characteristics. Hence, the discrete–time Rayleigh fading channel is frequency–nonselective (flat) and the input–output–relation reads

$$y[k] = g[k] \cdot x[k] + n[k] \ , \tag{1}$$

where the fading process $g[\cdot]$ and the noise process $n[\cdot]$ are mutually independent correlated and uncorrelated zero–mean complex Gaussian random processes with variances σ_g^2 and σ_n^2, respectively. For the autocorrelation function of the fading process the well–known Jakes fading model with maximum normalized Doppler frequency $f_d T$ (T: channel symbol interval) is used.

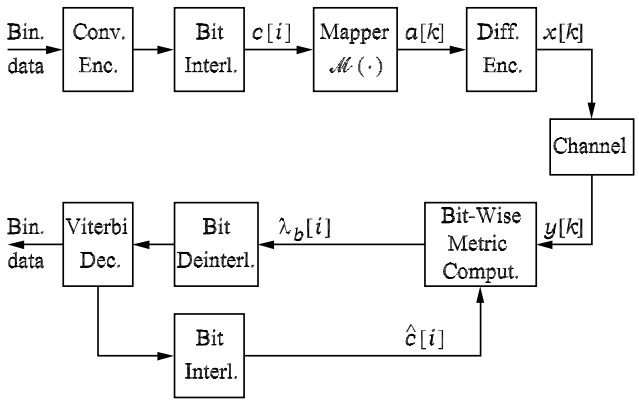

Figure 1: Discrete–time system model.

At the receiver, bit branch metrics $\lambda_b[i]$ are computed as described in Section 3. The deinterleaved metrics are the soft input for the standard Viterbi decoder. The *hard* decisions of the Viterbi decoder are interleaved and fed back to the metric calculation (cf. Figure 1) which now makes use of the previous decisions $\hat{c}[i]$. This procedure is repeated in a number of iterations.

3. Metric Calculation

Since the metric computation should incorporate the dependences between consecutive channel output symbols as completely as possible, $\lambda_b[i]$ is obtained using the complex N–dimensional probability density function (pdf) $p(\boldsymbol{y}[k]|\boldsymbol{a}[k])$ of $\boldsymbol{y}[k] \stackrel{\triangle}{=} [y[k], y[k-1], \ldots, y[k-N+1]]^T$ under the assumption $\boldsymbol{a}[k] \stackrel{\triangle}{=} [a[k], a[k-1], \ldots, a[k-N+2]]^T$, i.e, we base the metric on the observation of N received symbols. The pdf $p(\boldsymbol{y}[k]|\boldsymbol{a}[k])$ is derived in e.g. [17] for the flat Rayleigh fading channel.

Based on the pdf $p(\boldsymbol{y}[k]|\boldsymbol{a}[k])$ it is possible to compute the metrics for the $(N-1)\cdot\ell$ bits which via mapping bijectively correspond to one vector symbol $\boldsymbol{a}[k]$ as e.g. in [4]. Of course, in this case only observations $\boldsymbol{y}[k]$ at times $k = \kappa\cdot(N-1)$, $\kappa \in \mathbb{Z}$, overlapping each other by one received symbol are evaluated at the receiver. In contrast to this, we employ maximally overlapped observations $\boldsymbol{y}[k]$, cf. e.g. [14, 18]. That is, the metrics for ℓ bits, which label the scalar symbol $a[k]$, are calculated from the pdf values $p(\boldsymbol{y}[k]|\boldsymbol{a}[k])$. Optimally, M^{N-1} pdfs for all possible vectors $\boldsymbol{a}[k]$ have to be determined. Then, M^{N-1}/ℓ pdf calculations per bit metric are necessary, i.e., the computational effort grows exponentially with the observation length N.

Instead of considering all vector symbols $\boldsymbol{a}[k]$, we insert hard decision–feedback symbols $\hat{a}[k-\nu]$, $\nu = 1, 2, \ldots, N-2$, which considerably reduces the computational effort. Doing this, only M pdfs $p(\boldsymbol{y}[k]|a[k], \hat{a}[k-1], \ldots, \hat{a}[k-N+2])$ are necessary. This procedure is essentially the decision rule of DF–DD, e.g. [11], for uncoded transmission. The metric computation is further simplified if also $\ell-1$ decision–feedback bits, which belong to the label $a[k]$, are fed back. Then, only $\ell+1 < M = 2^\ell$ pdfs have to be determined since only $\ell+1$ different $a[k]$ are possible.

The μth bit, $\mu = 0, 1, \ldots, \ell-1$, of the label of $a[k]$ corresponds to the metric value $\lambda_b[i]$, where $i = k\cdot\ell+\mu$ holds. Subsequently, since the present symbol time index k is of no importance, we replace the index i by μ for clarity. Furthermore, the metric notation $\lambda_b[\mu]$ is completed by the subscript b, $b \in \{0, 1\}$, which gives the value of the considered bit. From the considerations above and assuming that the data symbols $a[k]$ are a priori equally likely, $\lambda_b[\mu]$ is given by

$$\lambda_b[\mu] = \log(p(\boldsymbol{y}[k]|\tilde{a}[k], \hat{a}[k-1], \ldots, \hat{a}[k-N+2])) \;, \quad (2)$$

where $\tilde{a}[k] = \mathcal{M}(\hat{c}[0], \ldots, \hat{c}[\mu-1], b, \hat{c}[\mu+1], \ldots, \hat{c}[\ell-1])$. Noteworthy, the number of branch bit metrics $\lambda_b[\mu]$ is independent of the observation length N, and identical to that for conventional differential demodulation. Because of the analogy to DF–DD and since the metrics constitute soft inputs for the decoder, we call this metric calculation strategy (2) *decision–feedback differential demodulation (DF–DM)*.

In order to save complexity it is reasonable to neglect all terms in the pdfs which do not depend on symbol $\tilde{a}[k]$. Then, $\lambda_b[\mu]$ can be simplified to [11]

$$\lambda_b'[\mu] = \mathrm{Re}\left\{\tilde{a}[k]y^*[k]\cdot\sum_{\nu=1}^{N-1} t_{0\nu}y[k-\nu]\prod_{n=1}^{\nu-1}\hat{a}[k-n]\right\} \;, \quad (3)$$

where $\mathrm{Re}\{\cdot\}$ denotes the real part of a complex number, and $t_{0\nu}$, $1 \le \nu \le N-1$, describes the fading statistics and is defined in equation (15) from [11].

Since a positive multiplicative or additive constant is of no importance for the decoding decisions in the Viterbi algorithm, it is possible to replace $t_{0\nu}$ by $p_\nu \stackrel{\triangle}{=} c\cdot t_{0\nu}$, $c \in \mathbb{R}^+$, $\nu = 1, 2, \ldots, N-1$, in (3). If c is chosen properly (cf. [11]), p_ν are the coefficients of a linear $(N-1)$st order minimum mean–squared error (MMSE) FIR predictor for the random process $g[\cdot] + n[\cdot]x^*[\cdot]$. In this case, these coefficients p_ν can be adaptively determined in a simple manner by employing, e.g., the recursive least–squares (RLS) algorithm [19, 20].

4. Iterative Decoding Algorithm

For DF–DD of uncoded MDPSK the feedback symbols $\hat{a}[k-\nu]$ stem from immediate decisions on transmitted symbols. When error correction coding and bit interleaving is applied, it is reasonable to obtain the decision–feedback symbols from the bit decisions $\hat{c}[i]$ of the Viterbi decoder via remodulation. Of course, for the first demodulation of a received sequence (first decoding iteration), no previous decisions $\hat{c}[i]$ are available. Then, in order to keep the demodulation as simple as possible, we resort to conventional differential demodulation based on two consecutive received symbols, i.e., $N = 2$. For the further demodulations (decoding iterations) remodulated feedback symbols $\hat{a}[k-\nu]$ and address bits $\hat{c}[\mu]$ are used in order to calculate bit branch metrics based on an observation interval $N > 2$. In Figure 2, the iterative DF–DM decoding algorithm is summarized.

Since with BICM after the first iteration by far the best performance is achieved if Gray labeling of data–carrying symbols $a[k]$ is used, we apply usual Gray labeling throughout this paper.

Bit metric calculation based on observation window $N=2$
Viterbi decoding
While maximum number of iterations is not achieved
Remodulation of bit decisions of the Viterbi decoder
Bit metric calculation based on observation interval $N > 2$
Viterbi decoding
Output bit decisions of the Viterbi decoder

Figure 2: The iterative DF–DM decoding algorithm.

Due to the iterative structure of the decoding algorithm the question of convergence arises. By regarding the demodulation with observation length $N > 2$ as an estimation problem it is analytically shown in [21] that the algorithm converges for usually desired bit error rates (BER).

5. Cutoff Rate for Genie–Aided DF–DM

A good trade–off between powerful error correcting coding and fair complexity of decoding is offered by application of convolutional codes and decoding with the Viterbi algorithm. For this coding scheme, the cutoff rate R_0 of the associated memoryless channel is a common measure of performance. Hence, R_0 for genie–aided DF–DM, i.e., all decision–feedback symbols are assumed to be correct, is used to judge the achievable performance of DF–DM for different window lengths N. Following the derivations in [13], we define the so–called average Bhattacharyya factor

$$B \triangleq \frac{1}{\ell} \sum_{\mu=0}^{\ell-1} \mathcal{E}_{b,\boldsymbol{y}} \left\{ \sqrt{\frac{\exp(\lambda_{\bar{b}}[\mu])}{\exp(\lambda_b[\mu])}} \right\} , \tag{4}$$

where $\bar{b}$ denotes the complement of b. The cutoff rate for BICM in bits per channel use is given by

$$R_0 = \ell \cdot (1 - \log_2(B+1)) . \tag{5}$$

Subsequently, this expression is numerically evaluated. Since genie–aided DF–DM is assumed, there is no dependence on the number of iterations.
First, cutoff rates for 4DPSK over $\bar{E}_s/N_0$ ($\bar{E}_s$: average energy per received signal, N_0: one–sided noise power spectral density) are considered. In Figure 3, the influence of the observation length N is examined for Jakes fading model with $f_dT = 0.01$. The curve for $N = 2$ represents the cutoff rate corresponding to conventional differential demodulation without decision–feedback. As reference curve and upper bound, the cutoff rate of coherent 4PSK with perfect channel state information (CSI) at the receiver is also shown. As can be seen, there is a relatively large potential gain in power efficiency by expanding the demodulation window from $N = 2$ to $N = 3$ for DF–DM. A further increase of N leads to a higher R_0 for given $\bar{E}_s/N_0$, but the improvements are comparatively small. This observation will be confirmed by simulation results in Section 6.

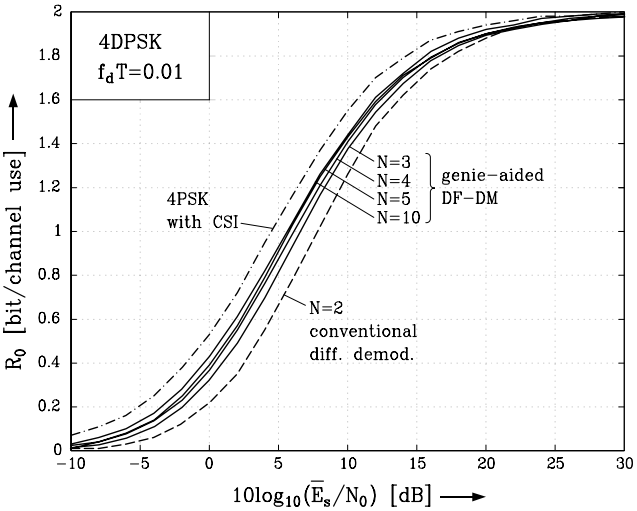

Figure 3: Cutoff rate for 4DPSK and Rayleigh fading with $f_dT = 0.01$. Dashed line: conventional differential demodulation with $N = 2$. Solid lines: genie–aided DF–DM with $N = 3, 4, 5, 10$. Dash–dotted line: 4PSK with perfect CSI.

For 8DPSK in Figure 4 the interaction between the fading rate f_dT and the achievable performance of 8DPSK with DF–DM is illustrated, where the respective cutoff rates for $f_dT = 0.001$ and $f_dT = 0.05$ are plotted. For slow fading ($f_dT = 0.001$), there is a steady improvement in terms of R_0 by increasing N. On the other hand, for fast fading ($f_dT = 0.05$), the gains expected from DF–DM depend strongly on the desired transmission rate. Here, DF–DM is most advantageous if high rate codes are employed, i.e., $R_0 \geq 2$ bit/(channel use). The flattening of the curve for $N = 2$ and $f_dT = 0.05$ at $R_0 \approx 2.15$ bit/(channel use) moves to values of about 2.8 bit/(channel use). This coincides with the results in [11] for uncoded DPSK transmission, where for differential detection with $N = 2$ an error floor is observed for fast fading, which is practically removed by DF–DD if N is chosen properly. For comparison, the cutoff rate for coherent 8PSK, which is independent of f_dT, of course, is also included in Figure 4. For slow fading, by increasing N, the cutoff rate for coherent 8PSK with perfect CSI is approached, whereas for fast fading, a considerable gap remains between the curves for coherent and noncoherent transmission. These analytical results are in great accordance with the simulation results presented in Section 6.

6. Simulation Results

In order to further assess the proposed iterative decoding scheme, simulations of the system in Figure 1 with flat Rayleigh fading have been performed. In this section, the measured BERs are presented as functions of $\bar{E}_b/N_0$ ($\bar{E}_b$: average energy per information bit). As for calculation of the cutoff rate, we concentrate on 4DPSK and 8DPSK transmission. For each transmitted BICM block, bit interleavers are randomly generated to obtain results which are independent of a particular interleaver.
For 4DPSK, the target rate of 1 bit/(channel use) is regarded as a relevant example, which is generated through the stan-

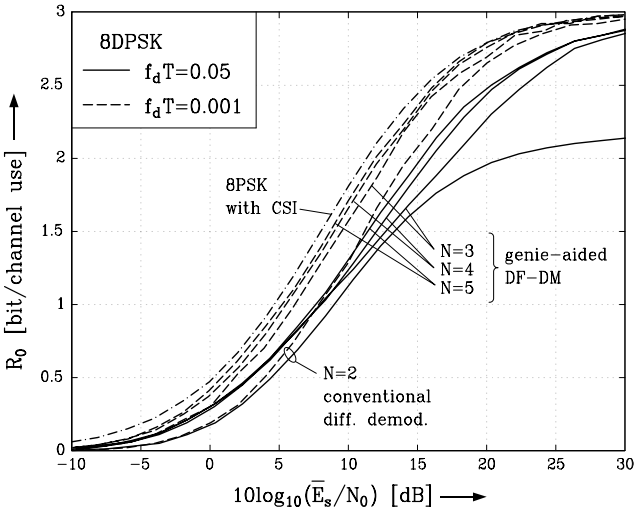

Figure 4: Cutoff rate for 8DPSK and Rayleigh fading. Conventional differential demodulation with $N = 2$ and genie–aided DF–DM with $N = 3, 4, 5$. Dashed lines: $f_dT = 0.001$. Solid lines: $f_dT = 0.05$. Dash–dotted line: 8PSK with perfect CSI.

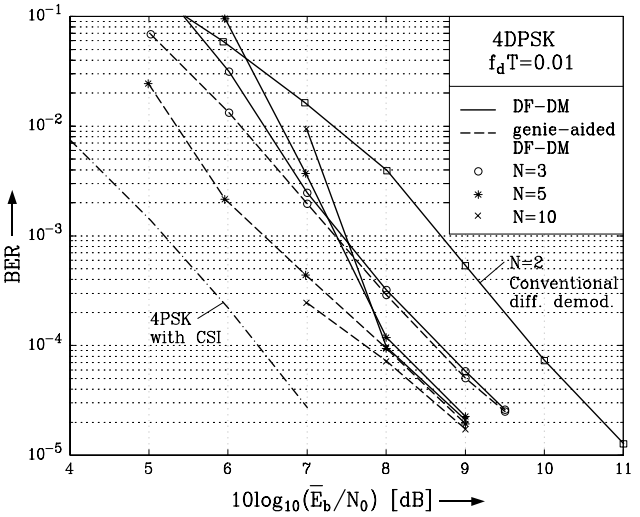

Figure 5: BER versus $10\log_{10}(\bar{E}_b/N_0)$ for 4DPSK and Rayleigh fading with $f_dT = 0.01$. 64 states convolutional code. DF–DM with four iterations. Solid lines: conventional differential demodulation with $N = 2$ and DF–DM with $N = 3, 5, 10$. Dashed lines: genie–aided DF–DM . Dash–dotted line: 4PSK with perfect CSI.

dard rate 1/2 convolutional code with 64 states and generator polynomials $(133, 171)_8$. The flat fading channel is specified by $f_dT = 0.01$. Bit interleaving over 4000 bits, which correspond to 2000 channel symbols, is applied in order to provide transmission diversity.

The performances of conventional differential demodulation, DF–DM with observation lengths $N = 3, 5, 10$, and coherent 4PSK with perfect CSI at the receiver are compared in Figure 5. For clarity of presentation, DF–DM with four iterations is only shown. Noteworthy, for $N = 3, 5$ almost identical BERs are obtained with only two and three iterations, respectively. As performance limits, the measured BERs for genie–aided DF–DM are also plotted. Due to erroneous feedback, the curves for DF–DM with $N = 3, 5, 10$ intersect. However, DF–DM provides considerable gains in power efficiency for a wide range of target BERs. The large gap in power efficiency between coherent and conventional differential demodulation is significantly reduced by the simple DF–DM scheme. About 1.8 dB can be gained for $\mathrm{BER} \leq 10^{-4}$. The simulation results coincide with the cutoff rate analysis (see Figure 3), where very similar performance gains are predicted. In particular, DF–DM with $N = 10$ is only marginally superior to DF–DM with $N = 5$ and code rate 1/2.

Now, more bandwidth efficient 8DPSK transmission with 2 bit/(channel use) is considered. The punctured rate 2/3 convolutional code with 64 states and generator polynomials $(135, 163)_8$ is taken. Both fast fading with $f_dT = 0.05$ and slow fading with $f_dT = 0.001$ are assumed. Appropriate bit interleaving of 3000 and 60000 bits, respectively, which correspond to 1000 and 20000 channel symbols, respectively, is performed.

In Figure 6, the simulation results for fast fading with $f_dT = 0.05$ are presented. For 8DPSK and differential demodulation with $N = 2$ a flattening of the bit error rate occurs, which leads to an extremely large performance loss for $\mathrm{BER} < 10^{-3}$ in comparison to coherent 8PSK with perfect CSI. By iterative DF–DM decoding, this flattening is removed. Thus, for $\mathrm{BER} \leq 10^{-3}$ huge performance gains are realized. Increasing the demodulation window N results in an improved power efficiency of 8DPSK transmission. But since relatively fast fading is present, a gap of about 4 dB to the case of perfect CSI remains as was to be expected from the cutoff rate analysis (cf. Figure 4).

For the case of 8DPSK and $f_dT = 0.001$ simulation results are plotted in Figure 7. Since the fading is relatively slow, the power efficiency of coherent 8PSK can be better approached by DF–DM (cf. also Figure 4). 8DPSK and DF–DM with $N = 5$ requires an SNR for $\mathrm{BER} \leq 10^{-4}$ which is only about 1 dB higher than the SNR for coherent transmission with perfect CSI. The gain of using DF–DM with $N = 5$ compared to usual differential demodulation amounts to about 2.2 dB. Noteworthy, also for 8DPSK the iterative decoding algorithm converges for the target BER's which are usually of interest.

7. Conclusions

MDPSK transmission over flat Rayleigh fading channels without channel state information at the receiver is considered. For the application of convolutional codes and bit interleaving, a novel simple iterative decoding procedure (DF–DM) is proposed, where hard decisions of the Viterbi algorithm are fed back in order to enlarge the demodulation window. This decoding procedure has the distinct advantage of requiring only a very moderate increase in computational complexity compared to conventional differential demodulation with observation length $N = 2$.

By a cutoff rate analysis the potential gains in power efficiency are quantified. It is shown that the achievable performance gains strongly depend on the transmission rate and the

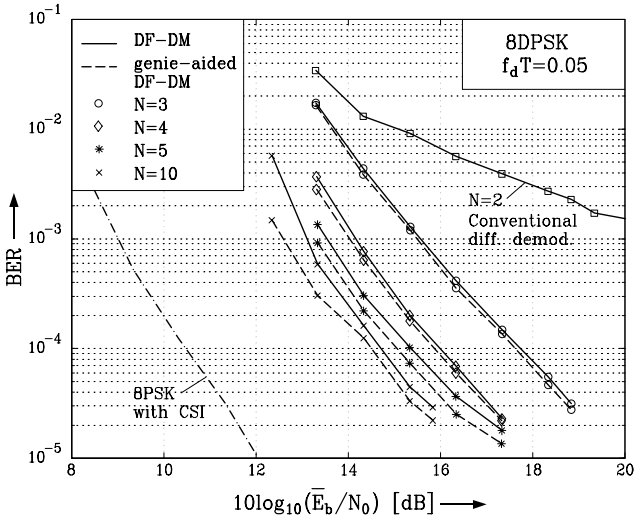

Figure 6: BER versus $10\log_{10}(\bar{E}_b/N_0)$ for 8DPSK and Rayleigh fading with $f_dT = 0.05$. 64 states convolutional code. DF–DM with four iterations. Solid lines: conventional differential demodulation with $N = 2$ and DF–DM with $N = 3, 4, 5, 10$. Dashed lines: genie–aided DF–DM. Dash–dotted line: 8PSK with perfect CSI.

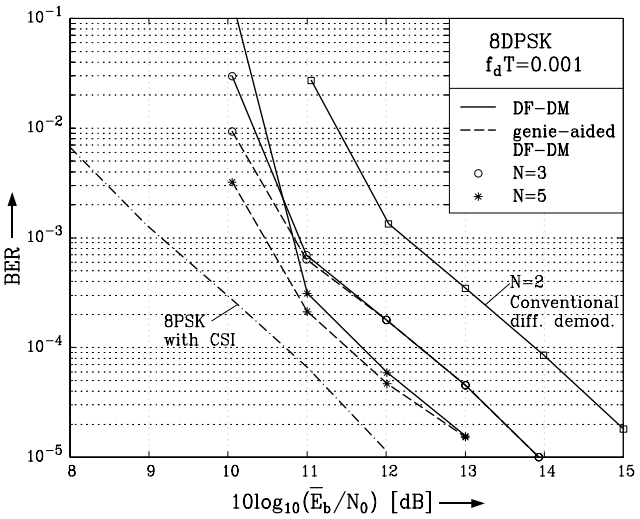

Figure 7: BER versus $10\log_{10}(\bar{E}_b/N_0)$ for 8DPSK and Rayleigh fading with $f_dT = 0.001$. 64 states convolutional code. DF–DM with four iterations. Solid lines: conventional differential demodulation with $N = 2$ and DF–DM with $N = 3, 5$. Dashed lines: genie–aided DF–DM. Dash–dotted line: 8PSK with perfect CSI.

fading rate.

The cutoff rate analysis is well confirmed by the presented simulation results. The iterative decoding shows convergence for usually desired BER's. Compared to conventional differential demodulation remarkable performance improvements are achieved. Thus, we believe that the proposed low complex iterative decoding algorithm with DF–DM is an interesting solution for a number of applications, e.g. mobile communications, where computational complexity is limited.

References

[1] D. Divsalar and M.K. Simon. Multiple–Symbol Differential Detection of MPSK. *IEEE Trans. Com.*, 38(3):300–308, March 1990.

[2] Y. Kofman, E. Zehavi, and S. Shamai (Shitz). *nd–* Convolutional Codes—Part I: Performance Analysis. *IEEE Trans. Inf. Theory*, 43(2):558–575, March 1997.

[3] M. Peleg and S. Shamai (Shitz). On the Capacity of the Blockwise Incoherent MPSK Channel. *IEEE Trans. Com.*, 46(5):603–609, May 1998.

[4] M. Peleg and S. Shamai (Shitz). Iterative Decoding of Coded and Interleaved Noncoherent Multiple Symbol Detected DPSK. *Electr. Letters*, 33(12):1018–1020, June 1997.

[5] M. Peleg and S. Shamai (Shitz). On Coded and Interleaved Noncoherent Multiple Symbol Detected MPSK. *Europ. Trans. Telecom. (ETT)*, 10(1):65–73, January/February 1999.

[6] P. Hoeher and J. Lodge. "Turbo DPSK": Iterative Differential PSK Demodulation and Channel Decoding. *IEEE Trans. Com.*, 47(6):837–843, June 1999.

[7] K.R. Narayanan and G.L. Stüber. A Serial Concatenation Approach to Iterative Demodulation and Decoding. *IEEE Trans. Com.*, 47(7):956–961, July 1999.

[8] I. D. Marsland and P. T. Mathiopoulos. On the Performance of Iterative Noncoherent Detection of Coded M–PSK Signals. *IEEE Trans. Com.*, 48(4):588–596, April 2000.

[9] T. May and H. Rohling. Turbo Detection of Convolutionally Coded and Differentially Modulated Signals. *Signal Processing*, 80:349–355, 2000.

[10] H. Leib and S. Pasupathy. The Phase of a Vector Pertubed by Gaussian Noise and Differentially Coherent Receivers. *IEEE Trans. Inf. Theory*, 34:1491–1501, November 1988.

[11] R. Schober, W.H. Gerstacker, and J.B. Huber. Decision–Feedback Differential Detection of MDPSK for Flat Rayleigh Fading Channels. *IEEE Trans. Com.*, 47(7):1025–1035, July 1999.

[12] E. Zehavi. 8–PSK Trellis Codes for a Rayleigh Channel. *IEEE Trans. Com.*, 40(5):873–884, May 1992.

[13] G. Caire, G. Taricco, and E. Biglieri. Bit–Interleaved Coded Modulation. *IEEE Trans. Inf. Theory*, 44(3):927–946, May 1998.

[14] Dan Raphaeli. Noncoherent Coded Modulation. *IEEE Trans. Com.*, 44:172–183, February 1996.

[15] G. Colavolpe and R. Raheli. Nonoherent Sequence Detection. *IEEE Trans. Com.*, 47(9):1376–1385, September 1999.

[16] X. Li and J.A. Ritcey. Trellis–Coded Modulation with Bit Interleaving and Iterative Decoding. *IEEE J. Select. Areas Commun.*, 17(4):715–724, April 1999.

[17] P. Ho and D. Fung. Error Performance of Multiple–Symbol Differential Detection of PSK Signals Transmitted over Correlated Rayleigh Fading Channels. *IEEE Trans. Com.*, 40:25–29, October 1992.

[18] G. Colavolpe and R. Raheli. Noncoherent Sequence Detection of M-ary PSK. In *Proc. IEEE Int. Conf. Commun. (ICC)*, pages 21–25, Montreal, June 1997.

[19] R.J. Young and J.H. Lodge. Detection of CPM Signals in Fast Rayleigh Flat–Fading Using Adaptive Channel Estimation. *IEEE Trans. Veh. Techn.*, pages 338–347, May 1995.

[20] R. Schober and W.H. Gerstacker. Decision-Feedback Differential Detection Based on Linear Prediction for MDPSK Signals Transmitted Over Ricean Fading Channels. *IEEE J. Select. Areas Commun.*, 18:391–402, March 2000.

[21] L.H.-J. Lampe and R. Schober. Decision–Feedback Differential Demodulation of Bit–Interleaved Coded MDPSK for Flat Rayleigh Fading Channels. *In revision: IEEE Trans. Com., 1999*.